Chinese Chemical Letters 32 (2021) 861–865

Contents lists available at ScienceDirect

Chinese Chemical Letters

journal homepage: www.elsevier.com/locate/cclet

Communication

Barium charge transferred doped carbon dots with ultra-high quantum yield photoluminescence of 99.6% and applications

Yao Liu[a,d,1], Jianfei Wei[b,1], Xiang Yan[c], Ming Zhao[d], Chaozhong Guo[a,*], Quan Xu[d,*]

[a] Chongqing Key Laboratory of Materials Surface & Interface Science, College of Materials Science and Engineering, Chongqing University of Arts and Sciences, Chongqing 402160, China
[b] School of Materials Designing and Engineering, Beijing Institute of Fashion Technology, Beijing 100029, China
[c] School of Materials Science and Engineering, Baise University, Baise 533000, China
[d] State Key Laboratory of Heavy Oil Processing, Beijing Key Laboratory of Biogas Upgrading Utilization, China University of Petroleum-Beijing, Beijing 102249, China

ARTICLE INFO

Article history:
Received 17 May 2020
Received in revised form 24 May 2020
Accepted 26 May 2020
Available online 30 May 2020

Keywords:
Ba-doped
Carbon dots
Quantum yield
Charge transfer
Fluorescent sensors

ABSTRACT

Long-emission carbon dots (CDs) is triggering immense enthusiasm on account of their intrinsic merits of high chemical stability and excellent optical properties. In this study, a facile and rapid approach was developed for the preparation of barium-doped carbon dots (Ba-CDs) with yellow fluorescence emission and high quantum yields. Surface chemistry and the chemical architecture of the Ba-CDs was revealed under various spectroscopic methods. This work provides more insights into the effects of charge transfer caused by Ba heteroatoms, which is considered as the most challenging step in the investigation on luminescence mechanism. Remarkably, the prepared Ba-CDs were successfully applied as fluorescent probes in the detection of trace water in organic solvents (ethanol, isopropanol, acetone, tetrahydrofuran). Comparing with traditional fluorescent probes for water detection in organic solvents, Ba-CDs detection provides a more sensitive, much faster and more economical approach.

Carbon dots (CDs), a new member of the fluorescent materials was first discovered in 2004 [1], showing a multitude of outstanding properties such as good photo-absorption, photostability and photobleaching resistance. The excellent and unique properties render them highly attractive for potential applications in areas of fluorescent printing [2,3], fluorescent probe [4–6], electrochemical catalyst [7,8] and light-emitting devices (LEDs) [9,10]. Previously, most efforts were put into improving the photoluminescence (PL) quantum yield (QY) of CDs. Numerous methods and a variety of raw materials were attempted in the synthesis of CDs [11,12]. In recent years, the surface passivation and heteroatom doping approaches have been proved very effective in terms of enhancing the properties of CDs. Consequently, CDs of significantly improved PLQY were reported and 94% yield was observed with blue emission [13]. Later, a sulfur doped CDs was created via simple hydrothermal treatment, and a 67% PLQY was achieved [14]. Zhu *et al.* reported a QY of 80% with N doped CDs [15]. Furthermore, metal heteroatoms were doped into carbon dots adjust to the electronic density and the resulting optical properties of carbon dots [16–22]. Previously, Qu and co-workers developed blue, green and orange emissive CDs through the employment of three different solvents [23]. Fan and co-workers reported a synthesis of blue, green, and red emission CDs (up to 52.6%, 35.1% and 12.9% QY) by controlled graphitization and surface function, realizing the tuning of emission from 430 nm to 630 nm [23]. Sun and co-workers demonstrated that emission of three colors at 340, 440 and 540 nm can be achieved with S, N, Co-doped graphene quantum dots at 61%, 45%, and 8% yield [24]. In addition, Yang's group was able to obtain long and near infrared emissive CDs (QY ≈ 30%) using dopamine and *o*-phenylenediamine as precursors [25]. Wang *et al.* prepared near-infrared emissive CDs with high quantum yield (QY) of 33.96% in an aqueous solution [26]. Meanwhile, triangular CDs from blue to red with a quantum yield up to 54%–72% have been reported [27]. Yang *et al.* also prepared CDs with blue dispersed emission and red aggregation-induced emission [28]. Despite these efforts, high photoluminescence CDs that can be easily synthesized and readily excited by long wavelength ($\lambda > 400$ nm) is highly desirable. To the best of our knowledge, the metal doped CDs with high PLQY (> 80%) reported showed emission entirely in the blue to green-light region only.

* Corresponding authors.
E-mail addresses: guochaozhong1987@163.com (C. Guo), xuquan@cup.edu.cn (Q. Xu).
[1] These authors contributed equally to this work.

https://doi.org/10.1016/j.cclet.2020.05.037
1001-8417/

Therefore, it is urgently needed to attain long- wavelength and high PLQY of CDs to broaden its application, especially in fluorescent probes, photocatalysis and LEDs fields. In addition, the PL mechanism of CDs is not clearly understood. Further study is in urgent need to extend the CDs emissions to longer wavelengths. In this work, yellow-emitting at long-wavelength fluorescent carbon dots doped with Ba were prepared through a facile one-step solvothermal method and high fluorescence quantum yield (up to 99.6%) was obtained. The sample of Ba-CDs showed an intense and distinct emission at 560 nm after being excited at 460 nm. So far, this is reported for the first time that Ba-CDs have achieved an over 90% PLQY of fluorescence at long wavelength ($\lambda > 500$ nm). Various spectroscopic techniques, including transmission electron microscopy (TEM), fluorescence spectroscopy, X-ray photoelectron spectroscopy (XPS) and FTIR were applied to reveal the surface chemistry and the chemical architecture of the Ba-CDs. The effect of Ba charge transfer doping and the fluorescence mechanism were studied. The synthesized Ba-CDs were used as water sensing fluorescent probe for the detection of water in organic solvents (ethanol, isopropanol, acetone, tetrahydrofuran). It was found that Ba-CDs displayed unique fluorescence properties that can be rapidly quenched by water. Based on the quenching effect observed in the presence of water, Ba-CDs fluorescence at 560 nm was used in the qualitative and quantitative analysis of trace water in ethanol, isopropanol, acetone, tetrahydrofuran organic solvents, achieving good linearity. Comparing with other fluorescent probes for water analysis in organic solvent, the fluorescent behavior of Ba-CDs eliminates the necessity of modifying water structure and provides effortless applications.

In this study, sodium citrate and urea were selected as carbon sources. The schematic synthesis process of the yellow luminescent Ba-CDs is shown in Fig. 1a. Spherical morphology was evidently revealed under the Transmission Electron Microscopic (TEM) investigations. According to the TEM images (Fig. 1b), Ba-CDs was synthesized uniformly and highly separated from each other. The high-resolution transmission electron microscopic (HRTEM) image inserted in Fig. 1c shows that notable crystalline characteristics were observed in a single quantum dot with a spacing of 0.21 nm. The result indicated the presence of (100) lattice planes of the graphitic carbon. A close look at the Ba-CDs disclosed that the quantum dots varied from 2.82 nm to 7.58 nm in size, with an average at around 4.95 nm (Fig. 1d). TEM-EDX analysis of Ba-CDs (Fig. 1e) and corresponding C, O, N and Ba elemental EDX mapping analysis of Ba-CDs (Figs. 1f–i) reveal the C content is 70.49 wt%, O content is 20.34 wt%, N content is 8.12 wt% and Ba content is only 1.04 wt% in Ba-CDs. The AFM image (Fig. S1 in Supporting information) further demonstrated the formation of mostly monodispersed *quasi* spherical Ba-CDs.

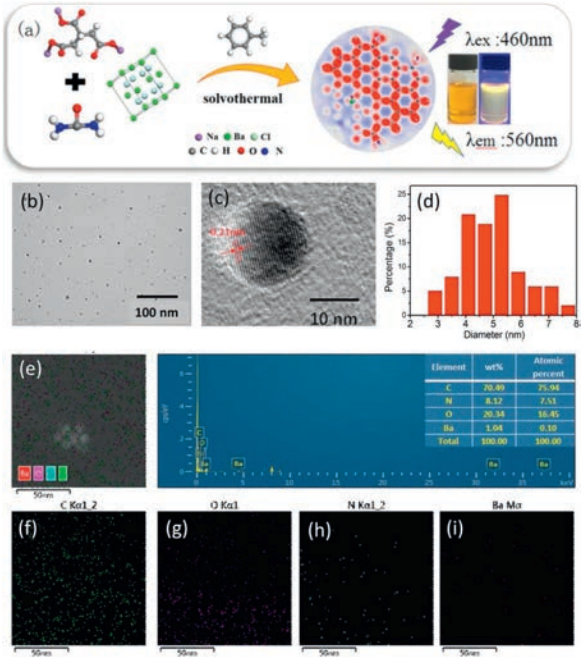

Fig. 1. (a) Schematic diagram of the synthesis process of yellow luminescent Ba-CDs. (b) TEM images of Ba-CDs. (c) The high resolution HRTEM images of the Ba-CDs. (d) The diameter distribution of Ba-CDs calculated from TEM image. (e) TEM-EDX analysis of Ba-CDs. (f) C, (g) O, (h) N and (i) Ba elemental EDX mapping analysis of Ba-CDs.

The optical properties of Ba-CDs were studied in detail. The sample was found to produce an absolute photoluminescence quantum yield up to 99.6% (Fig. S2 in Supporting Information). The emission characteristics of Ba-CDs were studied under irradiation with lights of varying wavelengths from 300 nm to 500 nm (Fig. S3a in Supporting Information). The contour plot is demonstrated in Fig. S3b (Supporting information). According to previous studies, reaction temperature and reaction time have significant impacts on the fluorescent properties of the carbon quantum dots [6]. The excitation spectrum ranges from 250 nm to 550 nm, the optimal λ_{em} at 460 nm. The optimal emission spectrum at 560 nm (λ_{ex} = 460 nm) of the Ba-CDs were presented in Fig. S3c (Supporting information). Comparison of known CDs and the Ba-CDs synthesized in this work in terms of emission wavelength and quantum yield (Tables S1 and S2 in Supporting information) indicates that the latter has highest quantum yield at long emission wavelength ($\lambda > 500$ nm) [9,23–25,27–33]. An important feature discovered was that the peak position of emission spectrum did not shift with the varying excitation wavelength, indicating that emission of Ba-CDs was independent of the excitation process. This observation was attributed to the highly homogeneous surface structure and the narrow distribution of Ba-CDs sizes. The UV–vis absorption spectrum of Ba-CDs (Fig. S3d in Supporting Information) exhibited two characteristic peaks. Absorption at 290 nm is ascribed to the formation of aromatic π orbitals on account of the formation of graphitic carbon structure [34], while the other peak at 440 nm is ascribed to the trapping of excited state energy by the surface states [35]. Fig. S3e (Supporting information) displayed the PL decay spectra of the Ba-CDs, and the photoluminescence lifetime is approximately 9 ns. Additionally, various microscopic and spectroscopic techniques were applied to the characterization of the morphology, structure, surface chemistry and photo-physics of the Ba-CDs synthesized under the optimum experimental conditions. The Raman spectra of the Ba-CDs was shown in Fig. S3f (Supporting information). Two predominant peaks can be observed at 1362 and 1582 cm^{-1}, which correspond to the D band and G band. The intensity ratio of D band to G band (I_D/I_G) is used to evaluate the disorder and graphitic degrees of carbon dots. A ratio of 0.38 readily tells that defected structures existed in Ba-CDs, which is partially responsible for the high quantum yield and the long-emission of Ba-CDs.

The contents of N, O, C, elements in Ba-CDs are surveyed from the XPS spectra by analyzing the peaks at 292.28 eV, 405.08 eV and 538.38 eV, respectively (Fig. S4a in Supporting information). The high-resolution C 1s band of the samples (Fig. 2a) can be deconvoluted into three peaks located at 284.5, 285.9 and 286.6 eV, which was assigned to sp^2 carbons C=C, C—N and C—O [36]. The N 1s (Fig. 2b), two peaks at 399.42 and 401.2 eV can be obtained after deconvolution, which was assigned to the pyridinic N and the pyrrolic N. The existence of N 1s peaks clearly indicates the successful doping of nitrogen into the carbon structure, which was also confirmed by the C 1s peaks. O 1s analysis of the XPS spectra (Fig. 2c) revealed two peaks located at 531.6 eV (C=O). To further gain insight into how the functional

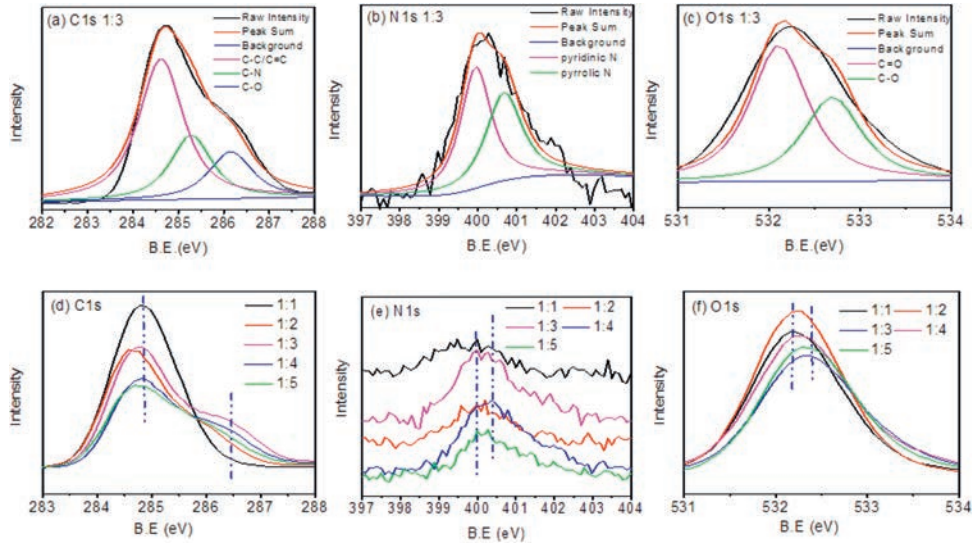

Fig. 2. High-resolution XPS (a) C 1s, (b) N 1s, (c) O 1s spectra for Ba-CDs. XPS (d) C 1s, N 1s, O 1s spectra of the five selected samples at different molar ratios of the urea and barium chloride.

groups or chromophore influence the photoluminescence, the high-resolution C 1s, N 1s and O 1s XPS spectra for other molar ratios of urea and barium chloride (1:1, 1:2, 1:4 and 1:5) were carefully examined (Figs. S5-S7 in Supporting Information). In terms of the C 1s peaks (Fig. 2d), the five CDs have a clear difference in the 286.6 eV peak. The Ba-CDs (1:3) has a distinct peak at C—O, while no peak was found for other samples, implying that the carboxyl carbons was intimately related to the photoluminescence and the high PLQY of the CDs. In the N 1s (Fig. 2e) XPS spectrum, the peaks of the as-prepared five samples all indicate the change in chemical state of nitrogen element from pyridinic N to pyrrolic N. The Ba-CDs (1:3) displays an outstanding pyrrolic N peak, which was one of the reasons for the high QY. Analysis of O 1s XPS spectra of these samples (Fig. 2f) found consistent result as C 1s analysis, confirming the improved content of sp^3 carbons in the Ba-CDs (1:3). The Ba 3d spectra of the five selected samples were shown in Fig. S8 (Supporting Information). However, inductively coupled plasma atom emission spectrometry (ICP-AES) analysis showed that the Ba content in the Ba-CDs (1:3) sample solution is 0.6090 mg/L.

The FTIR spectra further revealed the functional groups on the Ba-CDs (1:3) surface (Fig. S4b in Supporting information). A strong absorption at 3200 cm^{-1} correlates with the N—H stretching vibration. Absorption centered at about 2935 cm^{-1} is derived from the C—H stretching vibrations. C=N stretching contributes to the wide absorption at 1642 cm^{-1}. C=C stretching was discovered at 1524 cm^{-1}, showing that carbonization process is responsible for introducing the graphitic domains to the Ba-CDs. It is well known that element doping is an important reason for enhanced fluorescence quantum yield of CDs. Combining the analysis results of TEM-EDX, XPS, FTIR and ICP-AES, it is evident that Ba-CDs has a highly oxidized surface with the successful doping of Ba element.

To better understand the mechanism of heteroatom doping effect on CDs, we conducted first-principle calculations of doping element states in spherical modified CDs with Ba atom. From results it has been clearly demonstrated that the incorporation location of the impurity atom plays a critical role in regulating the properties of doped CDs. The electron density difference (EDD) distribution was calculated and shown in Figs. 3a–d. The EDD reflected the electron transfer between bonding atoms. The blue and red isosurfaces represent electron depletion and accumulation respectively in the chemical bond formation process. The oxygen site in the plot revealed vivid red since it features the highest electronegativity among those elements in pristine CDs and in Ba-CDs. The total densities of states (TDOSs) for the pristine CDs and Ba-CDs were calculated to reveal the effect of impurity doping on the electronic properties of CDs, which was illustrated in Fig. 3e. As can be observed, for Ba-doped cases, the Ba impurity-related peaks

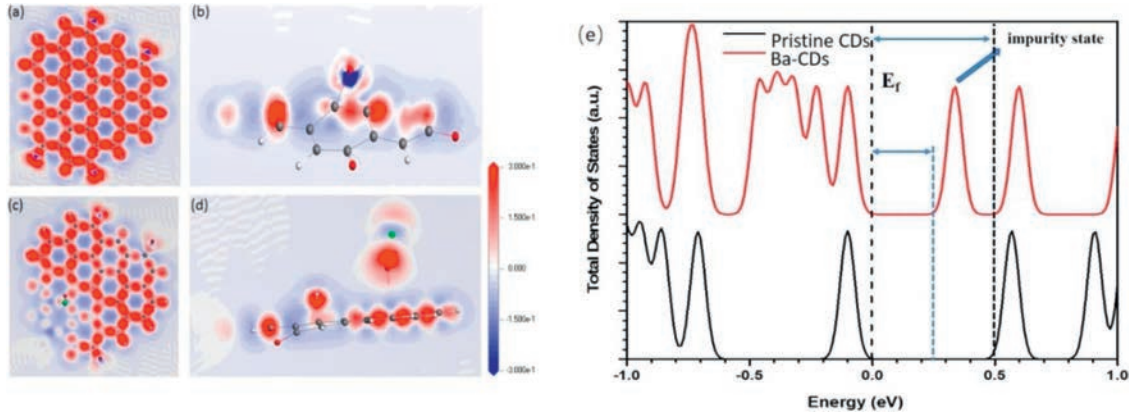

Fig. 3. (a) The top view the charge density of pristine CDs Ba-CDs. (b) The side view of the charge density of pristine CDs. (c) The top view the charge density of Ba-CDs. (d) The side view of the charge density of Ba-CDs. (e) Total density of states of pristine CDs and Ba-CD.

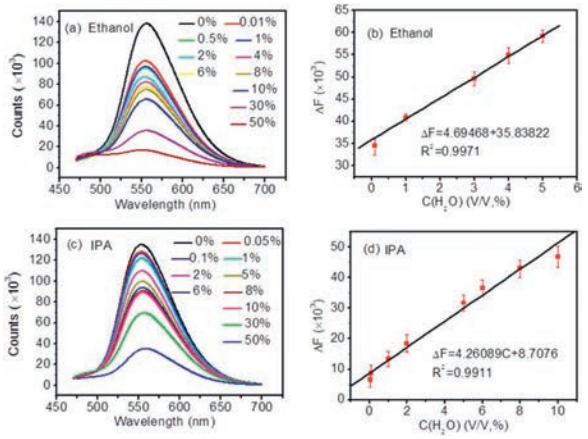

Fig. 4. (a) The fluorescence emission spectra of Ba-CDs dispersed in ethanol containing different concentration of H_2O. (b) Plot of ΔF against the concentration of H_2O from 0.01% to 5% in ethanol. (c) The fluorescence emission spectra of Ba-CDs dispersed in isopropanol containing different concentration of H_2O. (d) Plot of ΔF against the concentration of H_2O from 0.01% to 10% in IPA.

shifted towards LUMO as compared to pristine CDs, indicating the existence of Ba heteroatom generated an impurity state resulting in an elevated HOMO. Consequently, it significantly eases charge transfer, increases the lifetime of carriers, and thus improves quantum yield in Ba-CDs. As shown in Fig. S9 (Supporting information), the heteroatom Ba is loaded to CD by bonding to oxygen atom. There is no Ba bonding to C owing to the long distance between Ba and C atom. As shown in the Figs. 3b and d, negative charge density is found on Ba atom while positive charge density is found on O atom, indicating the charge transfer from Ba to O. Obviously enhanced blue colour, implying considerable electron depletion, was observed at Ba atom in Ba-CDs, corresponding to electron transfer from Ba to O. This demonstrates that charge transfer caused heteroatom is likely a reason for the high quantum yield in Ba-CDs.

The Ba-CDs are demonstrated as promising fluorescence "turn-off" sensors for low-level water Content in organic solvents. In this study, utilizing the unique fluorescence properties of Ba-CDs, we design the Ba-CDs as probes for detection of water in organic solvents. Fig. 4a shows a gradual decrease in fluorescence of Ba-CQDs when increasing the water content from 0 to 50% (v/v) in ethanol. The reduction in fluorescence was plotted against the amount of H_2O in Fig. 4b, where a good linearity with an excellent coefficient of determination ($R^2 = 0.9971$) was obtained when ΔF (the loss of PL intensity at 560 nm emission) was plotted against the concentration of H_2O ranging from 0.01% (v/v) to 10% (v/v). The time-dependent change (from 1 min to 10 min) in fluorescence of Ba-CDs in this solution system was also examined (Fig. S10a in Supporting Information). When repeating the same quantitative experiment in Ethanol, standard deviation in ΔF for five assays was sufficiently small, indicating a good reproducibility. The detection limit was determined to be as low as 0.001% ($DL = 3\sigma/k$), which is comparable to the previous results reported [37,38]. As aforementioned, Ba-CDs was used as florescent probes for the qualitative and quantitative determinations of trace water content in isopropanol, acetone and tetrahydrofuran. Fig. 4c showed the experimental results in isopropanol. The change in fluorescence intensity (ΔF) against the concentration of H_2O in isopropanol exhibited a good linear relationship in the range of 0–10% (v/v) (Fig. 4d). The linear equation is as follows: $\Delta F = 8.7076 + 4.26089C$ ($R^2 = 0.9911$), and the detection limit is as low as 0.0011%. Fig. S11a (Supporting information) showed the result of water content in acetone solution. ΔF and water concentration in acetone exhibited a good linear relationship in the range of 0–10%, as suggested by the linear equation: $\Delta F = 12.46948 + 15.32472C$, ($R^2 = 0.9951$), with the detection limit being 0.00035% (Fig. S11b in Supporting Information). Fig. S11c (Supporting information) showed the result in tetrahydrofuran solution determined by Ba-CDs. The quantitative relationship between ΔF and H_2O concentration is $\Delta F = 5.90201 + 16.34411C$ ($R^2 = 0.9918$), and the detection limit is 0.0033% (Fig. S11d in Supporting Information). Therefore, these experiments clearly demonstrated the strong potential of Ba-CDs in detecting water content in various kinds of organic solvents. Hence, the work provides a readily adaptable fluorescence-based protocol that has numerously potential applications in quality control of organic solvents. It has been reported that the absorption spectrum of the fluorophore changes during the static quenching process, while it remains constant during the dynamic quenching process [39–42]. Therefore, the absorption spectra of the fluorophore before and after quenching were compared. In Fig. S12 (Supporting information), the UV–vis absorption spectra of Ba-CDs and the Ba-CDs-water system were superposed with the experimental error, which indicates the dynamic quenching mechanism of the Ba-CDs-water system. Compared with the UV–vis absorption spectrum of Ba-CDs, the absorption peaks of Ba-CDs-water system at 290 nm and 440 nm have disappeared, indicating that the surface states and the graphitic carbon structure of Ba-CDs have been changed in the water system. In a word, the efficient quenching of fluorescence by water is attributed to the specific water–fluorophore interaction and partially to the increased solvent polarity when water is introduced.

In conclusion, we developed a facile and rapid approach for the preparation of Ba-CDs by solvothermal method. The carbon dots prepared gives off yellow fluorescence at ultrahigh PL yield. We conducted first-principle calculations of doping element states in spherical modified CDs with Ba atom and electron density difference to understand heteroatom doping effect mechanism on CDs. We infer that the charge transfer caused by heteroatoms is likely the reason for the high quantum yield in Ba-CDs, which are beneficial for the PL mechanisms of CDs. The products were applied to the analysis of organic solvents. It was the first time that Carbon Quantum Dots was applied as the fluorescent probe for the detection of low-level water impurity in organic solvents. It was found that the Ba-CDs have a unique and linear response to H_2O in organic solvents according to the luminescence results, achieving good correlation coefficients of 0.9971 (in ethanol), 0.9911 (in isopropanol), 0.9951 (in acetone), 0.9918 (in tetrahydrofuran), respectively. This work proposes a novel model to investigate the PL mechanisms for CDs and presents a readily adaptable fluorescence-based protocol with immense potential for applications in quality control of the solvent products.

Declaration of competing interest

The authors declare that they have no known competing financial interests or personal relationships that could have appeared to influence the work reported in this paper.

Acknowledgments

This study was financially supported by the National Natural Science Foundation of China (NSFC, No. 21805024), Science Foundation of China University of Petroleum (Nos. 2462019QNXZ02, 2462018BJC004), the Scientifc and Technological Research Program of Chongqing Municipal Education Commission (No. KJQN202001335), the Research Program of Yongchuan Science and Technology Commission (Ycstc, No. 2018nb1402).

Appendix A. Supplementary data

Supplementary material related to this article can be found, in the online version, at doi:https://doi.org/10.1016/j.cclet.2020.05.037.

References

[1] X. Xu, R. Ray, Y. Gu, et al., J. Am. Chem. Soc. 126 (2004) 12736–12737.
[2] W. Hui, Y. Yang, Q. Xu, Adv. Mater. (2019) 1906374.
[3] Q. Xu, W. Li, L. Ding, Nanoscale 11 (2019) 1475–1504.
[4] S. Chandra, D. Laha, A. Pramanik, et al., Luminescence 31 (2016) 81–87.
[5] Q. Xu, J. Zhao, Y. Liu, et al., J. Mater. Sci. 38 (2015) 9885–9890.
[6] Q. Xu, Y. Liu, C. Gao, et al., J. Mater. Chem. C 3 (2015) 9885–9893.
[7] W. Li, Z. Wei, B. Wang, et al., Mater. Chem. Front. 4 (2020) 277–284.
[8] H. Song, Y. Cheng, B. Li, et al., ACS Sustain.Chem. Eng. 8 (2020) 3995–4002.
[9] Z. Tian, X. Zhang, D. Li, et al., Adv. Opt. Mater. 5 (2017) 1700416.
[10] H. Song, X. Liu, B. Wang, et al., Sci. Bull. 64 (2019) 1788–1794.
[11] W. Li, Y. Liu, B. Wang, et al., Chin. Chem. Lett. 30 (2019) 2323–2327.
[12] P. Yang, S. Zhang, X. Chen, et al., Mater. Horiz. 7 (2020) 746–761.
[13] D. Qu, M. Zheng, L. Zhang, et al., Sci. Rep. 4 (2014) 5294.
[14] Q. Xu, P. Pu, J. Zhao, et al., J. Mater. Chem. A 3 (2015) 542–546.
[15] L. Zhou, P. Fu, Y. Wang, et al., J. Mater. Chem. A 4 (2016) 7222–7229.
[16] J. Du, Y. Zhao, J. Chen, et al., RSC Adv. 7 (2017) 33929–33936.
[17] Q. Xu, Y. Liu, R. Su, et al., Nanoscale 8 (2016) 17919–17927.
[18] S. Zhuo, Y. Guan, H. Li, et al., Analyst 144 (2019) 656–662.
[19] S. Sun, Q. Guan, Y. Liu, et al., Chin. Chem. Lett. 30 (2019) 1051–1054.
[20] N. Gong, H. Wang, S. Li, et al., Langmuir 30 (2014) 10933–10939.
[21] Z. Ye, R. Tang, H. Wu, et al., New J. Chem. 38 (2014) 5721–5726.
[22] V.B. Kumar, R. Kumar, A. Gedanken, et al., Ultrason. Sonochem. 52 (2019) 205–213.
[23] Q. Xu, M. Xu, C. Lin, et al., Adv. Sci. 6 (2019) 1902043.
[24] D. Qu, Z. Sun, M. Zheng, et al., Adv. Opt. Mater. 3 (2015) 360–367.
[25] S. Lu, L. Sui, J. Liu, et al., Adv. Mater. 29 (2017) 1603443.
[26] B. Wang, J. Li, Z. Tang, et al., Sci. Bull. (Beijing) 64 (2019) 1285–1292.
[27] F. Yuan, T. Yuan, L. Sui, et al., Nat. Commun. 9 (2018) 2249.
[28] H. Yang, Y. Liu, Z. Guo, et al., Nat. Commun. 10 (2019) 1789.
[29] P. Wang, C. Liu, W. Tang, et al., ACS Appl. Mater. Inter. 11 (2019) 19301–19307.
[30] C. Scialabba, A. Sciortino, F. Messina, et al., ACS Appl. Mater. Inter. 11 (2019) 19854–19866.
[31] W. Cai, T. Zhang, M. Xu, et al., J. Mater. Chem. C 7 (2019) 2212–2218.
[32] L. Sciortino, A. Sciortino, R. Popescu, et al., J. Phy. Chem. C 122 (2018) 19897–19903.
[33] M. Zhang, R. Su, J. Zhong, et al., Nano Res. 12 (2019) 815–821.
[34] R. Purbia, S. Paria, Biosens. Bioelectron. 79 (2016) 467–475.
[35] H. Li, C. Sun, M. Atieh, et al., Angew. Chem. Int. Ed. 54 (2015) 8420.
[36] L. Guo, J. Ge, W. Liu, et al., Nanoscale 8 (2016) 729–734.
[37] Y. Zhang, D. Li, Y. Li, et al., Chem. Sci. 5 (2014) 2710–2716.
[38] Y. Ooyama, S. Aoyama, K. Furue, et al., Dye. Pigment. 123 (2015) 248–253.
[39] S. Huang, L. Wang, C. Huang, et al., Sensor. Actuat. B -Chem. 221 (2015) 1215–1222.
[40] Z. Li, T. Wang, F. Zhu, et al., Chin. Chem. Lett. 31 (2020) 783–786.
[41] P. Yang, S. Zhang, X. Chen, Mater. Horiz. 7 (2020) 746–761.
[42] Z. Wang, Y. Zou, Y. Li, Small 43 (2020) 1907042.